International Journal of Mechanical, Industrial and Aerospace Sciences
ISSN: 2517-9950
Vol:9, No:1, 2015

Investigation and Perfection of Centrifugal Compressor Stages by CFD Methods

Y. Galerkin, L. Marenina

***Abstract*—**Stator elements «Vane diffuser + crossover + return channel» of stages with different specific speed were investigated by CFD calculations. The regime parameter was introduced to present efficiency and loss coefficient performance of all elements together. Flow structure demonstrated advantages and disadvantages of design. Flow separation in crossovers was eliminated by its shape modification. Efficiency increased visibly. Calculated CFD performances are in acceptable correlation with predicted ones by engineering design method. The information obtained is useful for design method better calibration.

***Keywords*—**Vane diffuser, return channel, crossover, efficiency, loss coefficient, inlet flow angle.

NOMENCLATURE

b	width of channel
c	flow velocity
D	diameter
M	Mach number
p	pressure
R	radius of curvature
Re	Reynolds number
T	temperature
u	circumferential velocity
V	volume flow rate
y+	dimensionless height of the first boundary-element
ε	compressibility factor
ζ	loss coefficient
η	efficiency
μ	dynamic viscosity
ρ	density
φ	flow rate coefficient
Φ	flow rate coefficient

Abbreviations, Subscripts, and Superscripts:

2, 3, 4, 5, 0′	indices of control sections
des	design
st	stator
*	stagnation parameters
CFD	Computational Fluid Dynamics
CR	crossover
SE	stator elements
IMP	impeller
RC	return channel
VD	vane diffuser
VLD	vane less diffuser

Yuri Borisovich Galerkin is with S.-Peterbugd Poltechnical Yniversity, Russian Federaton (phone: +7-921-942-73-40; fax: 8-812-552-86-43; e-mail: yuiri_galerkin@ mal.ru).

Lybov Nikolaevna Marenina is with S.-Peterbugd Poltechnical Yniversity, Russian Federaton (phone: +7-812-552-86-43 fax: 8-812-552-86-43; e-mail: lyubasic@mail.ru).

I. OBJECTIVE

ACCUMULATION of information about flow structure, detection zones of elevated pressure losses; improvement of stator elements in order to reduce pressure losses; update design recommendations (the choice of the optimal correlation of sizes); improvement of gas dynamic characteristics calculating methods.

The objects of research are stator elements of five intermediate stages with different specific speed, designed in accordance with the recommendations of [1] and optimized by the 4th generation computer programs [2]. The diffusers relative width of the five stages (b_3 / D_{2-3}): - 0,06, 0,047, 0,045, 0,041, 0,039. Diameter ratios: D_3 / D_{2-3}= 1, D_4 / D_{2-3}= 1,34, D_6 / D_{2-3}= 0,62 are the same for all stages.

Meridian configuration of the stage with the largest b_3 / D_{2-3} = 0,06 and control sections are shown in Fig. 1.

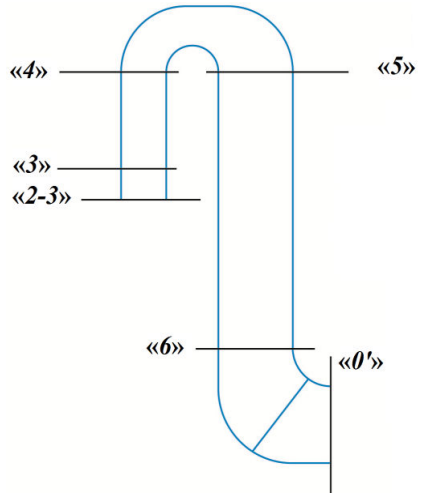

Fig. 1 Meridional configuration of the stage №1 and control sections

Stator elements include vaneless part, vane diffuser and return channel comprising a crossover, vane part, and the output axisymmetric confusor with straightener blades.

II. METHOD OF CALCULATION

Numerical calculations are performed using the software package ANSYS CFX 14. To create a three-dimensional model the program BladeGen was used. Grids were created by the program TurboGrid. Return channel vanes have an even number of main blades and half the number of straightening blades. The number of VD blades for the first four stages 23,

for the fifth stage - 19, the input and output angles of the first and second stages are $\alpha_{b3} = 21^0$, $\alpha_{b4} = 31{,}5^0$, for the third and fourth $\alpha_{b3} = 19^0$, $\alpha_{b4} = 31^0$, for the fifth $\alpha_{b3} = 15{,}5^0$, $\alpha_{b4} = 31^0$. The number of blades is not divisible by the number of blades of RC. The sector for the calculation of VD and RC respectively are equal to 15,65 (18,95 for the fifth stage) and 15°.

The computational domain for a VD single vane sector includes vaneless part and vane diffuser. It consists of 665 112 elements. The computational domain for it is built separately for one vane sector of main blades and RC blades and then combining into a single computational domain. The first part includes crossover, main blade and the part of the gap between main and straightening blades. It consists of 1 460 324 elements. Another part of the calculated area for RC contains a second part of the gap between blades, straightening blade and output part, consist of 907 200 elements. Around the blade is meshed C-type, the rest computational domain is a grid of H-type.

The position of the inlet and outlet boundaries in accordance with the recommendations of [3] is located on the "reasonable" distance from the front of the blade grid. To increase the accuracy of calculations the thickened grid is in the vicinity of the inlet and outlet edges of the blade.

Increasing the number of cells of the computational grid increases the accuracy of calculations. However, this process has a "saturation line" or, in other words, leads to the grid independence. The total number of elements of the computational domain mesh is 5 158 072. All calculations were made with the turbulence model *SST* [4]; y^+ values not exceed 10.

Inlet flow parameters correspond to the typical stages of industrial compressors:

- $M_{c3} = 0{,}588$,
- Reynolds number range for widest – narrowest stages is $\mathrm{Re}_{b3} = \frac{c_3 \cdot 2b_3 \cdot \rho_3}{\mu} = 1460\,000 \ldots 950\,000$.

Calculation was made for inlet flow angle values in the section *2-3:* 5, 7, 10, 15, 17, 18, 20, 22 degrees.

The value of polytrophic efficiency for SE as a whole is:

$$\eta = \frac{\ln\left(p_{0'} / p_{2-3}\right)}{\frac{k}{k-1}\ln\left(T_{0'} / T_{2-3}\right)}. \quad (1)$$

Corresponding value of the loss coefficient that is followed from Bernoulli's equation:

$$\zeta = (1-\eta)\left[1-\left(\frac{c_{0'}}{c_{(2-3)}}\right)^2\right]. \quad (2)$$

III. Efficiency Parameters

It is sufficient to know any two of the three dimensionless quantities η, ζ, $c_{0'} / c_{(2-3)}$ to calculate flow parameters at the outlet of the SE. Gas dynamic characteristics are presented as function of a flow angle α_{2-3}. The regime dimensionless parameter as an argument of η, ζ functions is introduced below.

Stage stator part can be coupled with impellers with different flow rate and work coefficients. It is important that the flow direction at section *2-3* was corresponding to minimum of loss coefficient at a design flow rate. Dimensionless regime parameter of stator elements - flow rate coefficient of stator elements ϕ_{st} – is introduced as follows. The continuity equation relates the stage flow rate coefficient with flow parameters at the inlet of SE:

$$\bar{m} = \Phi \frac{\pi}{4} D_2^2 u_2 \rho_0^* = 4\pi D_{2-3} b_{2-3} c_{r\,2-3} \rho_{2-3}. \quad (3)$$

Meaning that $c_{r\,2-3} = c_{u\,2-3} \cdot tg\alpha_{2-3}$ is possible to connect two main dimensionless parameters of impeller design Φ_{des}, ψ_{Tdes} [1] with the optimal angle of SE operation:

$$\phi_{st\,des} = \left(\Phi \frac{\rho_0^*}{\rho_{2-3}} / \psi_T\right)_{des} = 4\bar{b}_{2-3}\, tg\alpha_{(2-3)opt} \quad (4)$$

Formally, the stator elements and impeller with parameters corresponding to (4) may constitute a compressor stage. The additional condition the next one/ In accordance with [1], the ratio of vane heights of diffuser and impeller should be in the range $b_{2-3} / b_2 =$ 1,0-1,4. If this ratio does not correspond to (6), for the impeller SE with another angle $\alpha_{(2-3)opt}$ is necessary. To represent gas dynamic characteristics of all studied stages the argument ϕ_{st} is applied.

IV. Flow Structure

Flow pattern near leading edges of the stage #1 at tree inlet angles is shown at Fig. 2 (above) – radial surface on the mean height of blades. Angle $\alpha_{2-3} = 17°$ corresponds to the optimal regime. The optimal incidence angle is $i_{opt} = \alpha_{3bl} - \alpha_{2-3} = 21 - 17 = 4^0$.

Streamlines at Fig. 2 (below) show that at the angle $\alpha_{2-3} = 7^0$, incidence angle 14^0, the flow is fully separated. The local separation appears at the pressure side of blades when the angle $\alpha_{2-3} = 22^0$, incidence angle -1^0.

Fig. 3 shows the shear stresses on the pressure and suction surfaces of the VD vanes. Flow separation corresponds to regions of low shear stress (blue). The red zone on the suction surface at $\alpha_{2-3} = 22^0$ points on high level of friction losses.

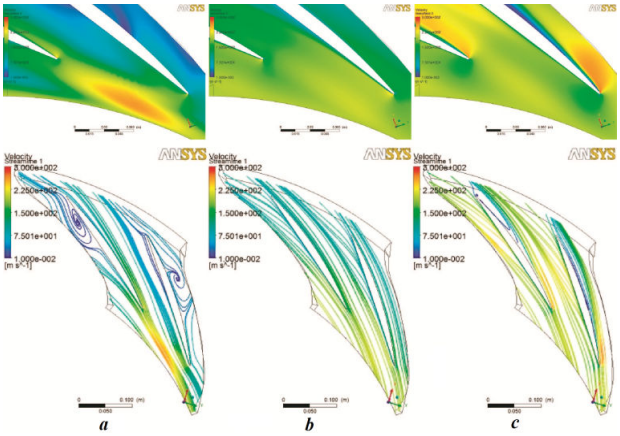

Fig. 2 Velocity field near the leading edge and streamlines at an average height of the blade surface in the VD (stage №1): (a) α_{2-3} = 7°; (b) α_{2-3} = 17°; (c) α_{2-3} = 22°

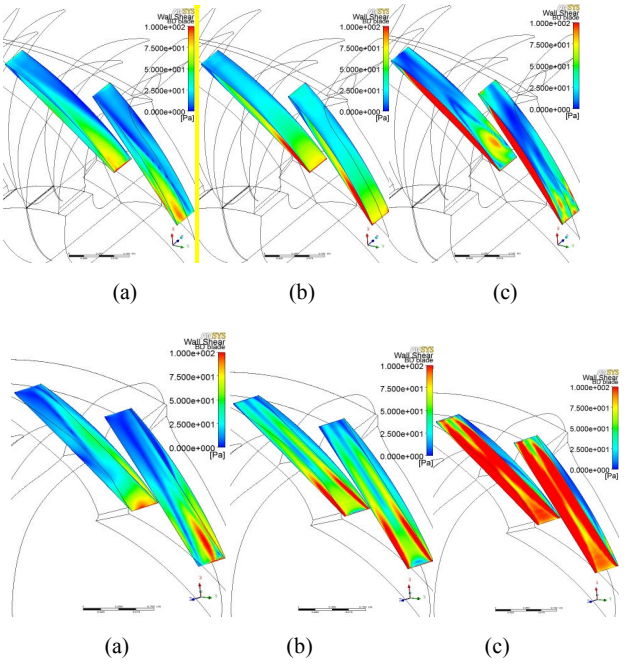

Fig. 3 Fields of shear stresses on the VD blade surfaces (stage №1). At the top - the pressure surfaces, at the bottom - the suction surfaces (a) α_{2-3} = 7°; (b) α_{2-3} = 17°; (c) α_{2-3} = 22°

Streamlines in the return channel at Fig. 4 show that the different level of separation takes place at all three inlet angles.

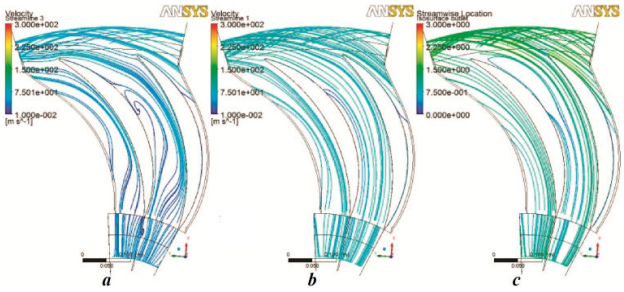

Fig. 4 Streamlines at an average height of the blade surface in the RC (stage №1): (a) α_{2-3} = 7°; (b) α_{2-3} = 17°; (c) α_{2-3} = 22°

The flow deceleration in RC is $c_0/c_4 \approx 0{,}90$. Evidently, it is possible to avoid separation with better flow organization. The streamlines in the meridian plane are shown in Fig. 5.

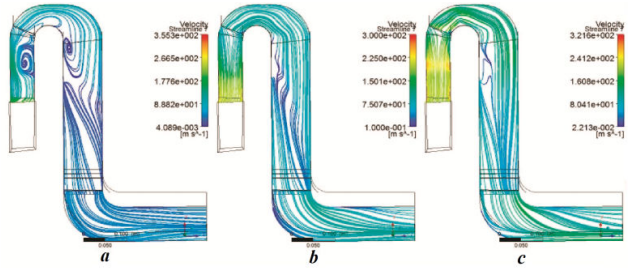

Fig. 5 Streamlines in the meridian plane of the RC (stage №1): (a) α_{2-3} = 7°; (b) α_{2-3} = 17°; (c) α_{2-3} = 22°

Flow pattern is not quite favorable even at optimal mode. According to the date presented in [1] a separation is not expected in the crossover if the inner radius of curvature $R_s/b_4 \geq 0{,}6$ - as in the stages ## 1- 5. Obviously, the used for design Universal modeling computer program of the 4th generation is not quite precise to predict flow behavior. It overestimates the importance of friction losses. The ratio b_5/b_6 = 1,0 was recommended by the program calculation. The flow deceleration in the crossover is too intensive as result. The crossover outlet/inlet ratio b_5/b_4 is about 2,0 that leads to flow separation.

V. Performance Curves

Fig. 6 shows the characteristics $\eta, \zeta = f(\alpha_{2-3})$ of the stator elements of the stage №1.

Reference [5] describes how to calculate the characteristics by the formulas with approximate estimation for compressibility. Obviously, the approximate calculation gives values significantly overestimates the pressure loss at M_{c3} = 0,588. Approximate ratio should be used in calculating the SE operating at low Mach numbers when (2) is invalid, say, at $M_{c3} \leq 0{,}3$.

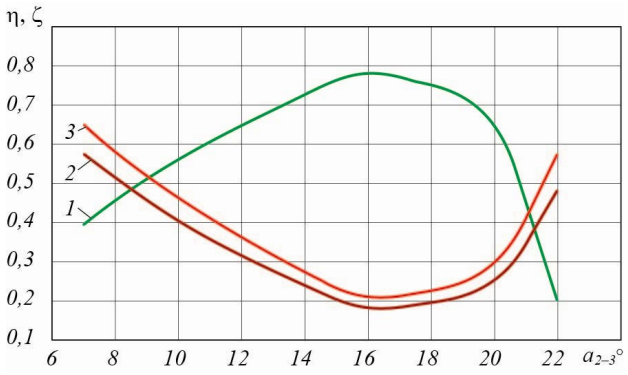

Fig. 6 Characteristics of the stator elements VD + RC (stage №1, «2-3» –« 0'»"): 1 - Efficiency; 2 - loss coefficient by (2); 3 - loss coefficient for incompressible flow [5]

Fig. 7 shows the characteristics of the efficiency and loss coefficients of SE of stages.

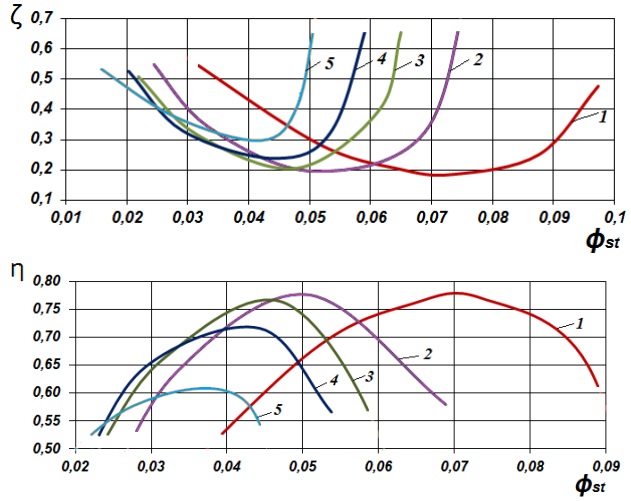

Fig. 7 Stator elements characteristics (section «2-3» –« 0'»") depending on the flow rate coefficient ϕ_{st}. 1 – $\bar{b}_{2-3}$ = 0,06; 2 $\bar{b}_{2-3}$ = 0,047; 3 – $\bar{b}_{2-3}$ = 0,045; 4 – $\bar{b}_{2-3}$ = 0,041; 5 – $\bar{b}_{2-3}$ = 0,039

The level of efficiency of the investigated elements cannot be considered particularly high. Shortcomings in the organization of the meridional flow have been shown above. Decrease of efficiency of the narrowest SE №5 is drastic. The optimal value the flow rate coefficient of SE #5 is ϕ_{st}~0,038. It is only twice less than the value for SE #1. The efficiency loss $\Delta\eta_{min} = 1 - \eta_{max}$ for SE #5 is 0,41 that is almost twice more than for SE #1. The cause of reduced efficiency is high friction losses on hub and shroud surfaces in narrow channels.

Fig. 8 shows the gas dynamic characteristics of the vane diffusers.

Efficiency of stage №1 vane diffuser (~83,5%) with a maximum specific speed and the loss coefficient (~0,125) correspond to the results of experiments and calculations by the Universal modeling method.

Fig. 9 shows the characteristics of RC loss coefficient.

Meridian form of RC stages of maximum (№ 1, $\bar{b}_{2-3}$ = 0,06) and minimum width (№5, $\bar{b}_{2-3}$ = 0,039) were modified for better organization of meridian flow. Modification was made by increasing the inner radius of curvature of crossover by reducing the height of the blades $\bar{b}_5$.

Modification yielded positive results. Effect of modification on the flow structure is shown in Fig. 10.

Flow meridian structure in SE №1 before modification is shown in Fig. 5. In the modified stages flow separation no occurs at the resign flow rate. In modified SE a meridian flow separation appears only at the extreme flow rates.

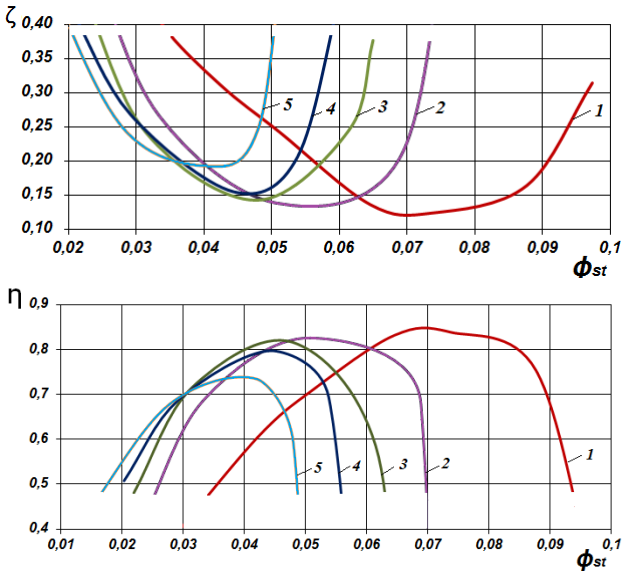

Fig. 8 Vane diffusers gas dynamic characteristics (section «2–3» – «4») depending on the conditional flow rate coefficient of stator elements ϕ_{st}. 1 – $\bar{b}_{2-3}$ = 0,06; 2 $\bar{b}_{2-3}$ = 0,047; 3 – $\bar{b}_{2-3}$ = 0,045; 4 – $\bar{b}_{2-3}$ = 0,041; 5 – $\bar{b}_{2-3}$ = 0,039

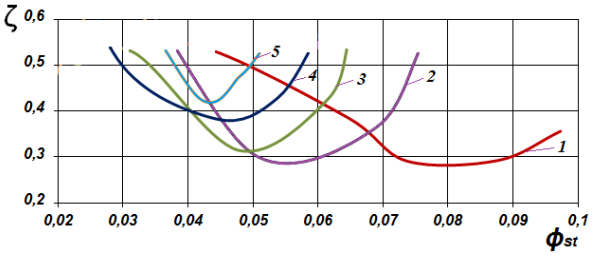

Fig. 9 Performance curves of RC loss coefficient, stages №№1 -5, 1 - stage №1; 2 - stage №2; 3 - stage №3; 4 - stage №4; 5 - stage №5

Fig. 11 demonstrates how modification has improved gas dynamic characteristics of SE № 1.

Maximum efficiency of SE № 1 has been increased by 1,6% due to the increase of the inner radius of CR curvature and the reduction ratio b_5/b_4.

Stator elements № 5 have improved efficiency by 2,6%, despite the fact that in narrow SE friction losses predominate.

VI. Performance Curves Validation

Fig. 12 demonstrates loss coefficient characteristics comparison calculated by ANSYS CFX and predicted by 4th generation modeling program.

The engineering type program prediction is good enough at design flow rates. Minimum loss coefficient on the "viscous" calculation is a little less for SE №№ 1-3. The opposite situation is for SE № 5. The right part of the characteristics match unsatisfactory. The SE calculations helped to improve flow path configuration and give information for calibration of engineering calculations.

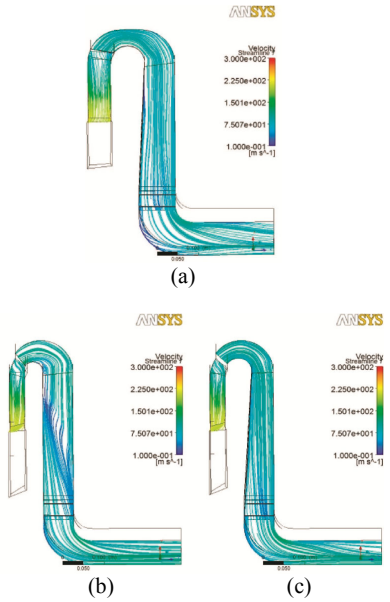

Fig. 10 Streamlines in the meridian plane of SE № 1 after modification (a). SE № 5 before modification (b) and SE № 5 after modification (c). Optimal flow rate

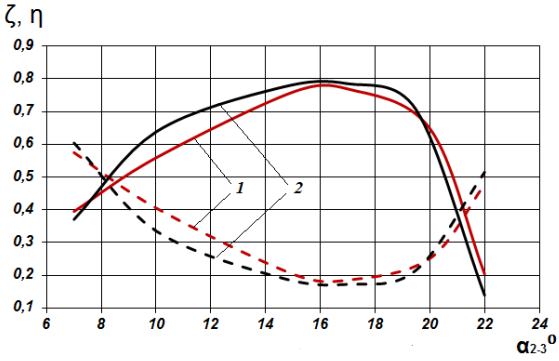

Fig. 11 Efficiency and loss coefficient of SE № 1 (section «2–3» – «0»') before (1) and after (2) modification

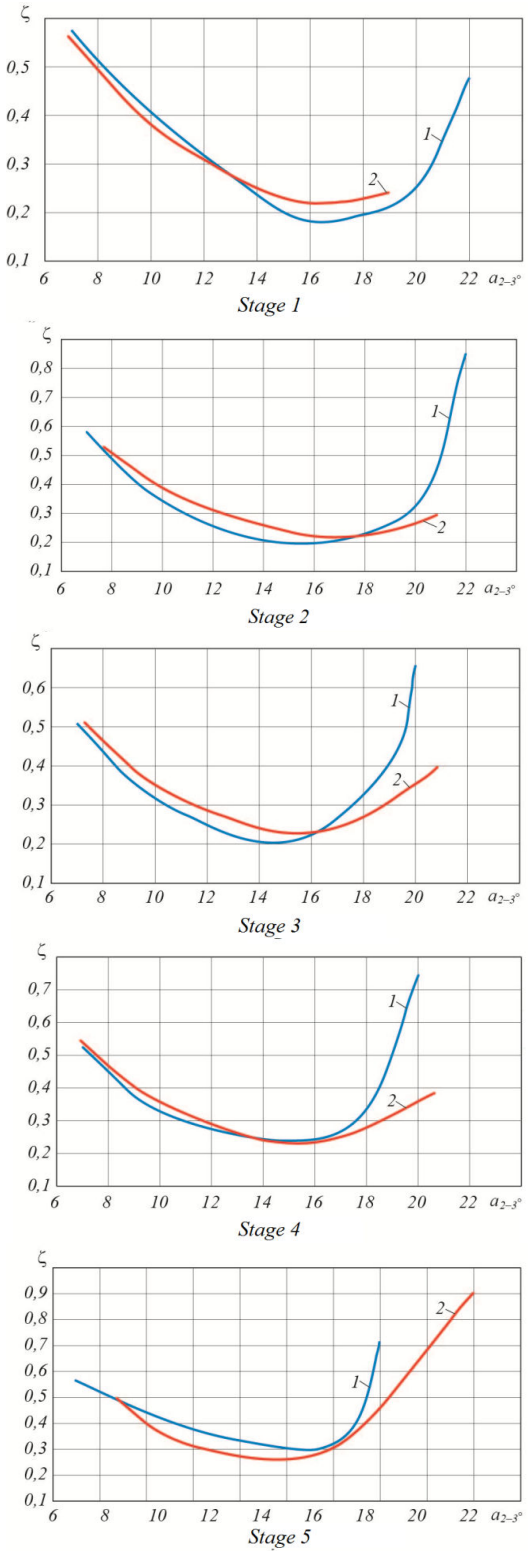

Fig. 12 Performance curves of loss coefficients SE №№ 1–5. 1 - ANSYS CFX; 2 - 4th version of the Universal modeling method

REFERENCES

[1] Y.B. Galerkin. Turbo compressors. // LTD information and publishing center. - Moscow. – KHT. -2010. - 596 p. (in Russian).
[2] Y.B. Galerkin, K.V. Soldatova, Operational process modeling of industrial centrifugal compressors. // Saint-Petersburg. - SPbTU. – 2011. - 328 p. (in Russian).
[3] S.A. Galaev. Numerical simulation of viscous flow in axial turbo machinery blade cascades: methodology and results of the application of modern software. Ph.D. thesis. SPb.: STU, 2006. 166 p. (in Russian)
[4] D.M. Gamburger. Numerical modelling of viscous flow in a centrifugal compressor stage: technique and results: Ph.D. thesis - TU SPb, 2009. - 190 p..
[5] Y.B. Galerkin, O.A. Solovieva. Improvement of vaneless diffusers calculation based on CFD experiments. Part 1 // Compressors and pneumatics, 2014. – № 3. (in Russian).